Electronic Supplementary Material (ESI) for RSC Advances.

Supporting Information

Enhanced catalytic activity of inhomogeneous Rh-based solid-solution alloy nanoparticles

Md. Samiul Islam Sarker[*, †], Takahiro Nakamura[*, ‡], Satoshi Kameoka[‡], Yuichiro Hayasaka[§], Shu Yin[‡], and Shunichi Sato[‡]

[†]Department of Physics, University of Rajshahi, Rajshahi-6205, Bangladesh.

[‡]Institute of Multidisciplinary Research for Advanced Materials (IMRAM), Tohoku University, Katahira 2-1-1, Aoba-ku, Sendai, 980-8577, Japan.

[§]Institute for Materials Research (IMR) Tohoku University, Katahira 2-1-1, Aoba-ku, Sendai, 980-8577, Japan.

*Corresponding authors

Email: nakamu@tohoku.ac.jp, samiul-phy@ru.ac.bd

1. Elemental distributions of RhPd and RhPdPt alloy nanoparticles

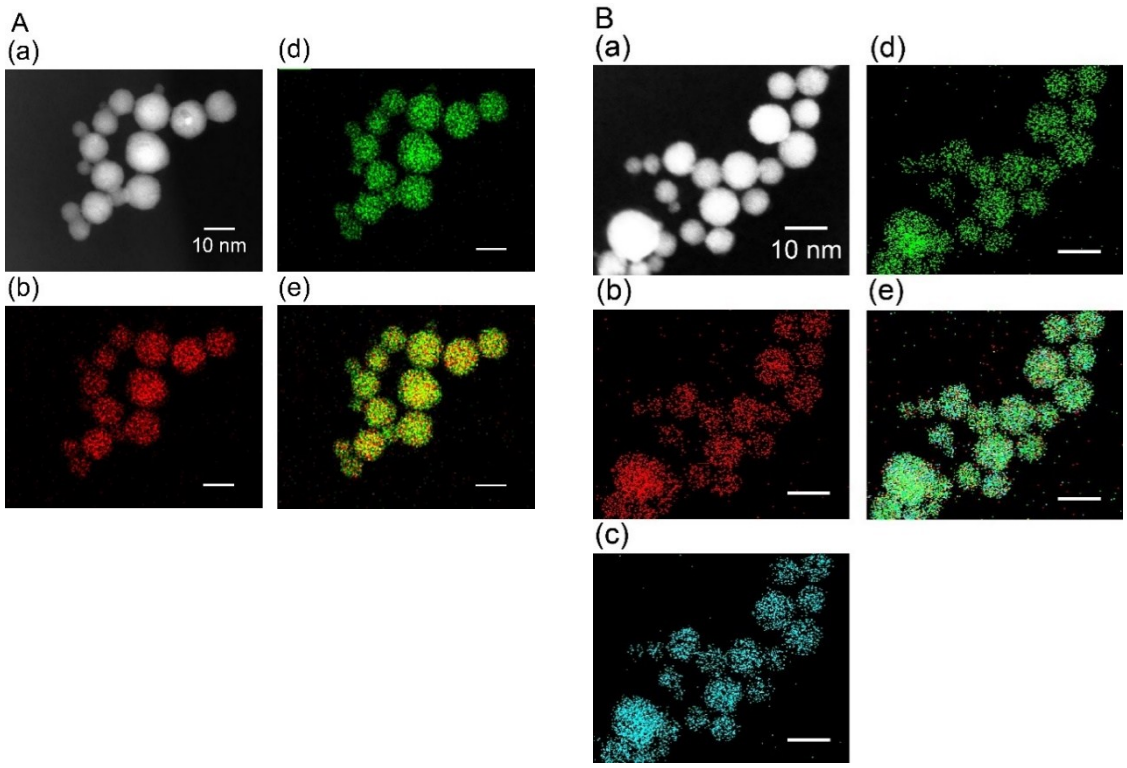

Figure S1. STEM-EDS elemental mappings of the nanoparticles fabricated in (A) RhPd and (B) RhPdPt solutions. (a) HAADF-STEM images; (b) Rh-L, (c) Pt-L, and (d) Pd-L STEM-EDS mappings; and (e) reconstructed image of the maps.

2. Local crystalline structure of the fabricated nanoparticles in the RhPd solution

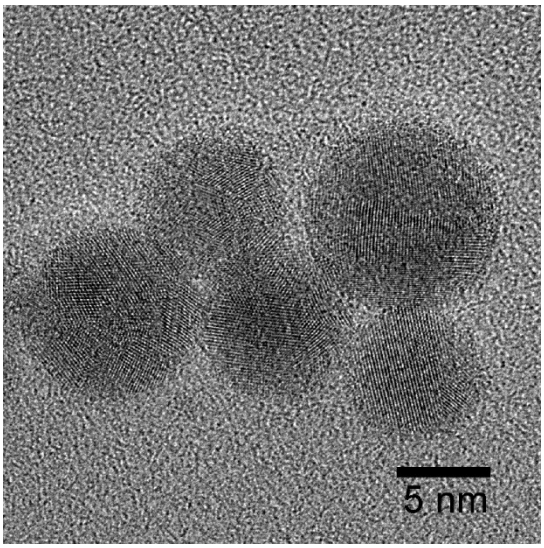

Figure S2. HR-TEM images of the nanoparticles fabricated in the RhPd solution.

3. XPS spectra of Rh, Pd and Pt for Rh–Pd–Pt alloy NPs

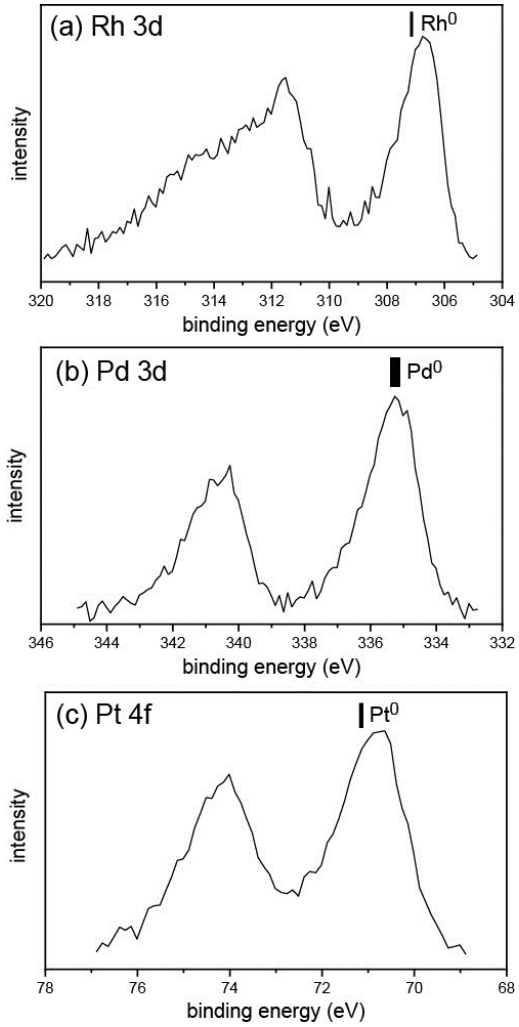

Figure S3. XPS spectra of (a) Rh, (b) Pd and (c) Pt for RhPdPt alloy NPs. The electric statuses of corresponding metals were also indicated in the spectra.

4. Supported catalysts

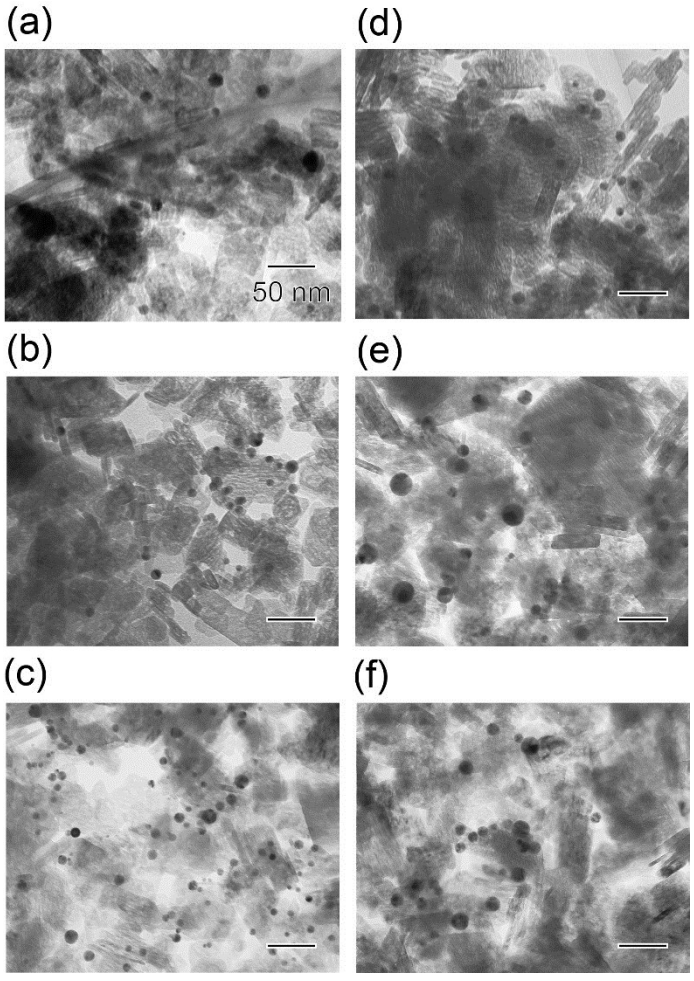

Figure S4. TEM images of the γ-Al_2O_3 supported catalysts. (a) Rh, (b) Pd, (c) Pt, (d) Rh–Pd, (e) Rh–Pt, and (f) Rh–Pd–Pt nanoparticles.

5. Catalytic stability of metal and alloy nanoparticle catalysts

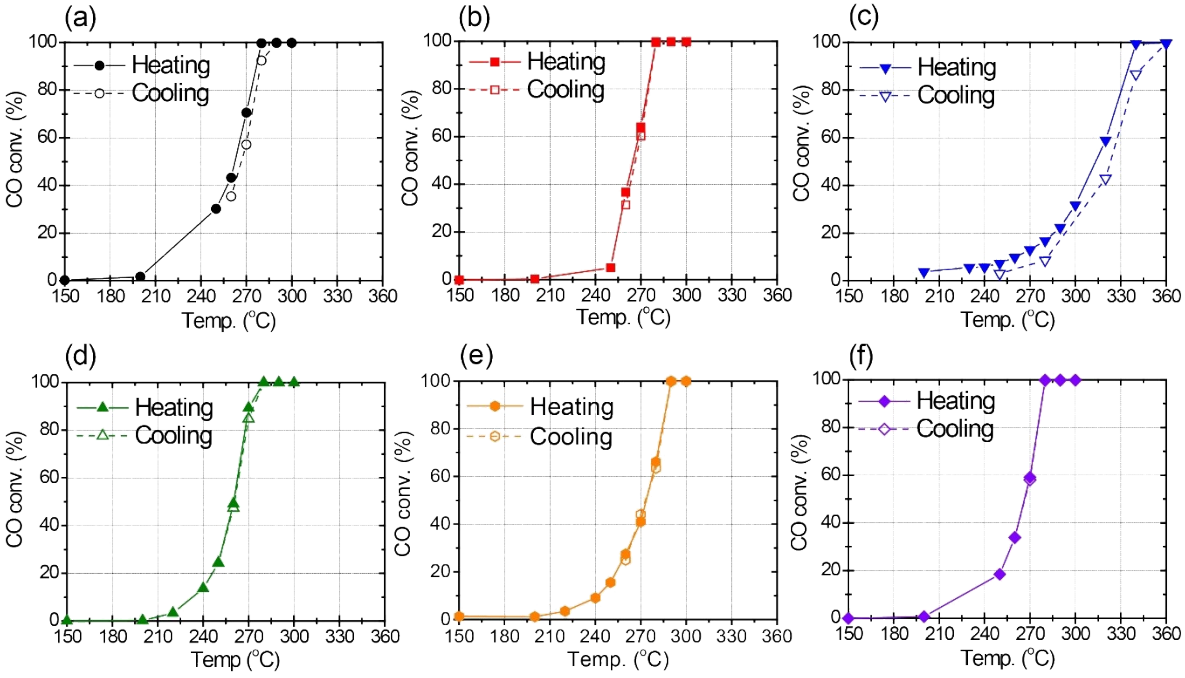

Figure S5. Catalytic stability of the as-prepared nanoparticle catalysts during CO conversion measured by hysteresis analyses during the heating and cooling process. (a) Rh, (b) Pd, (c) Pt, (d) RhPd, (e) RhPt, and (f) RhPdPt.

6. Supported catalysts after catalytic reaction

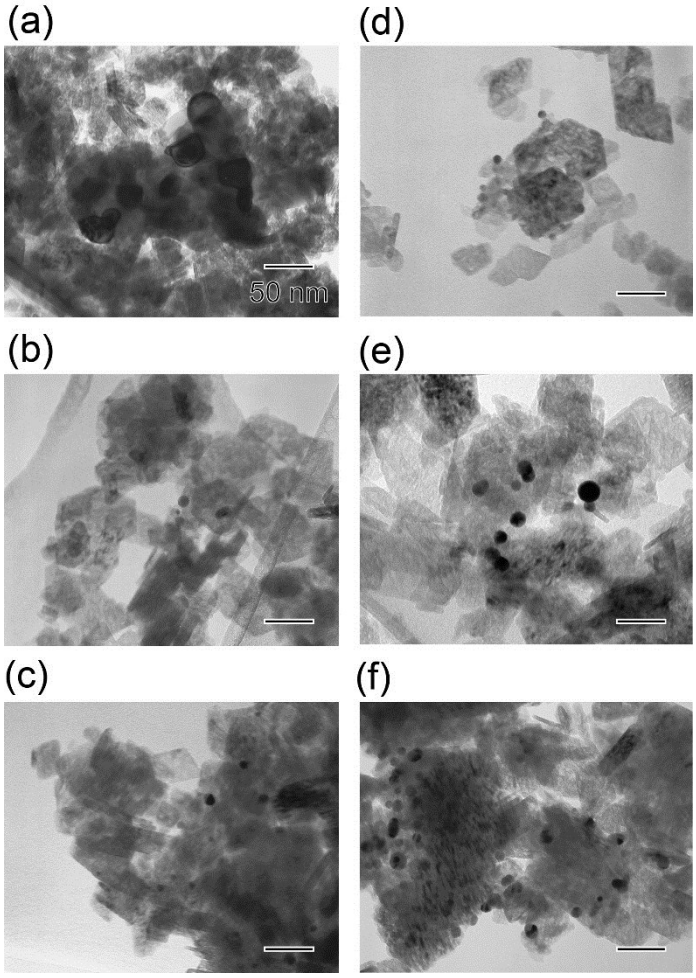

Figure S6. TEM images of the γ-Al_2O_3 supported catalysts after measurement of catalytic activities. (a) Rh, (b) Pd, (c) Pt, (d) RhPd, (e) RhPt, and (f) RhPdPt nanoparticles.

7. Elemental distributions of the alloy nanoparticle catalysts after catalytic reaction

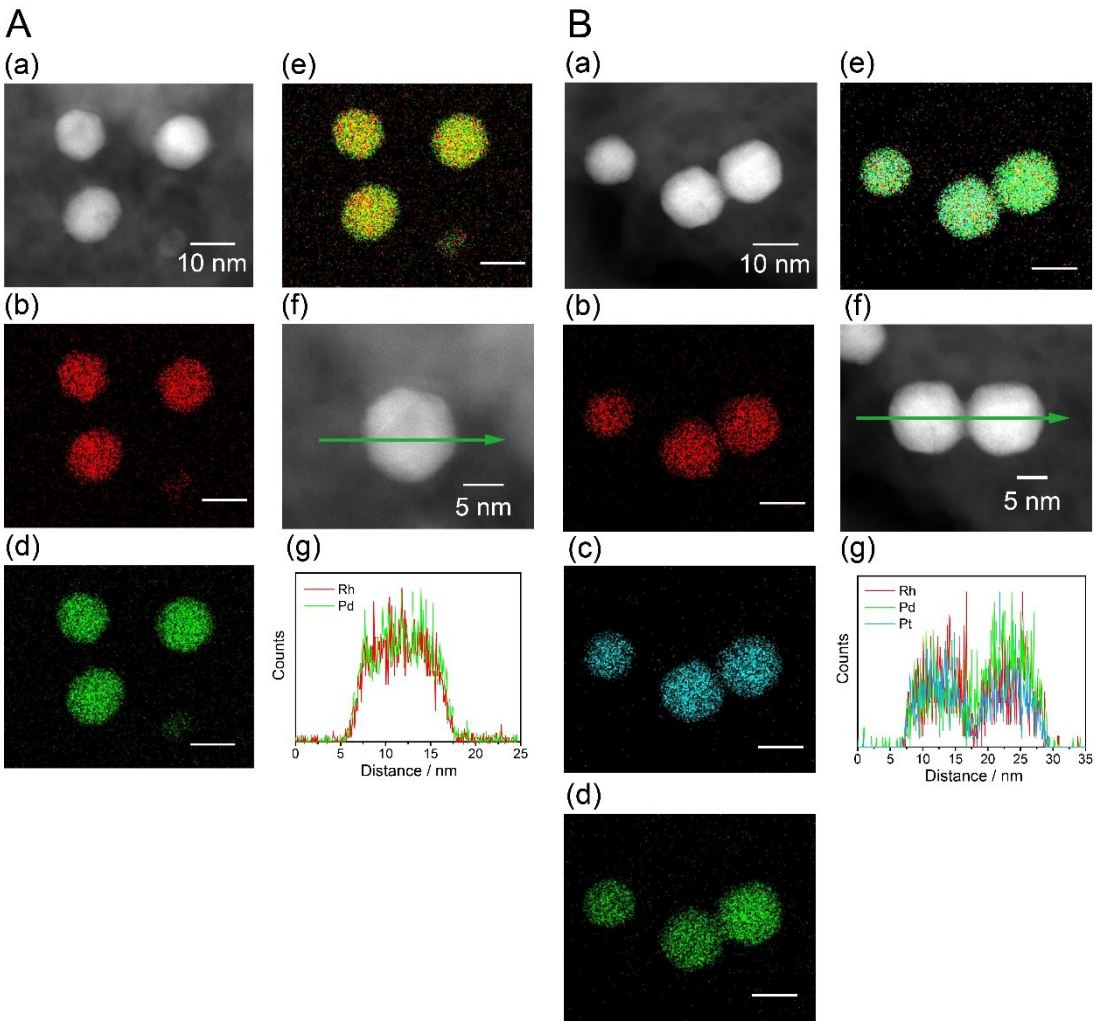

Figure S7. STEM-EDS elemental mappings of (A) RhPd, and (B) RhPdPt alloy nanoparticle catalysts after catalytic reaction. (a) HAADF-STEM images; (b) Rh-L, (c) Pt-L, and (d) Pd-L STEM-EDS mappings; and (e) reconstructed images of the maps in b, c, and d; (g) EDS line profile of Rh, Pd, and Pt for the nanoparticles along the green arrow in the STEM image (f).

8. Elemental distributions of alloy nanoparticle catalysts after heat-treatment

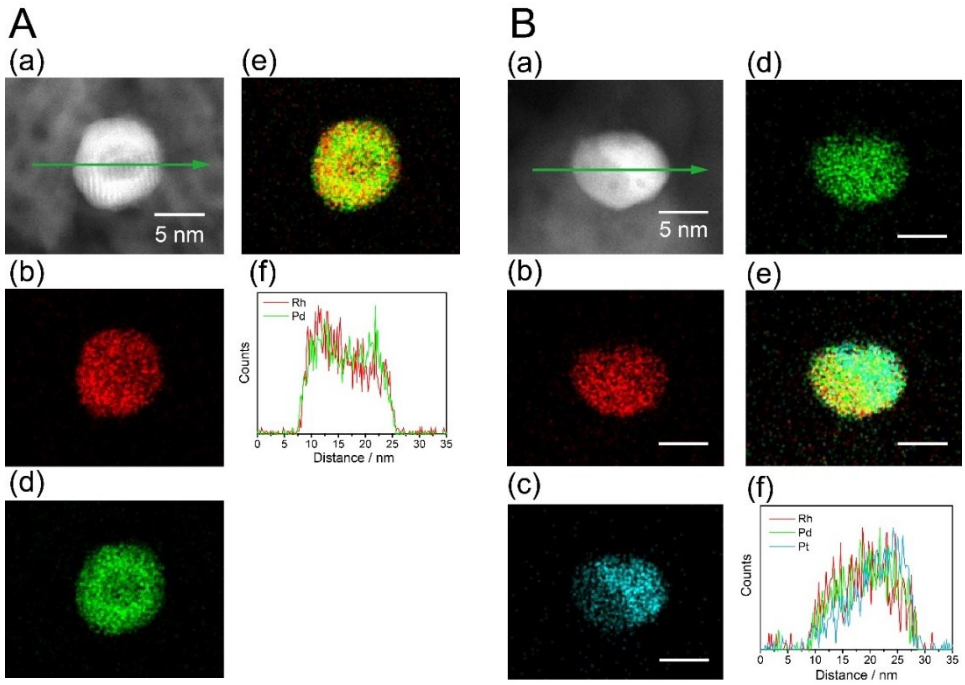

Figure S8. STEM-EDS mapping of the (A) RhPt and (B) RhPdPt alloy nanoparticles after heat-treatment of the homogeneous alloy nanoparticles. (a) HAADF-STEM image; (b) Rh-L, (c) Pt-L, and (d) Pd-L STEM-EDS mappings; (e) Reconstructed images of the maps shown in (b), (c), and (d); (f) EDS line profile of Rh, Pd, and Pt alloy nanoparticles along the green arrow in the STEM image shown in (a).

9. Catalytic stability of alloy nanoparticle catalysts after heat-treatment

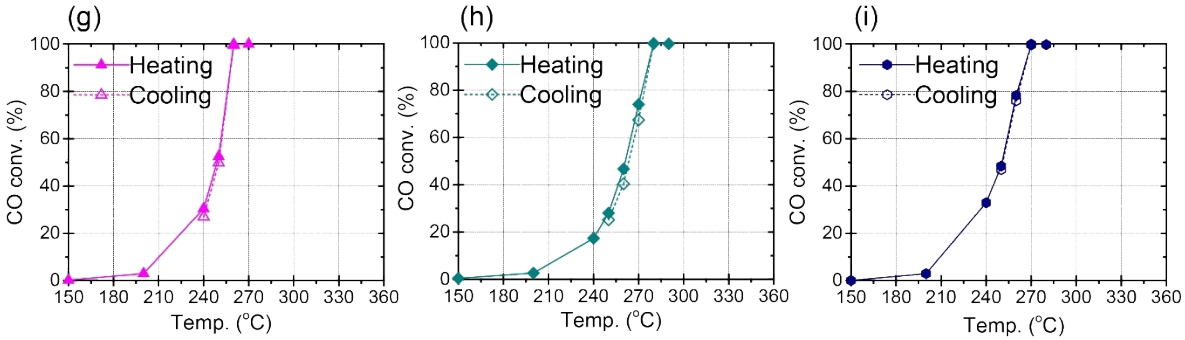

Figure S9. Catalytic stability of heat-treated nanoparticle catalysts during CO conversion measured by hysteresis analyses during the heating and cooling processes. (a) RhPd (b) RhPt, and (c) RhPdPt.